Magnetic susceptibility distribution in the soils of Pune Metropolitan Region: implications to soil magnetometry of anthropogenic loading

S. J. Sangode[1,*], K. Vhatkar[1], S. K. Patil[2], D. C. Meshram[1], N. J. Pawar[1], S. S. Gudadhe[1], A. G. Badekar[1] and V. Kumaravel[2]

[1]Department of Geology, University of Pune, Pune 411 007, India
[2]K.S. Krishnan Geomagnetic Research Laboratory (IIG), Chamanganj, Allahabad 221 505, India

Based on established linkages between ferrimagnetism and heavy metal concentration of anthropogenic particulates, we attempt here to delineate pollutant residing domains and study the role of surface runoff and wind circulations over its redistribution in the Pune Metropolitan Region (PMR) in Maharashtra. A total of 118 samples collected in a ~3 × 3 km grid during pre- and post-monsoon seasons for surface soils, bedrock, dust and rainwaters were analysed for magnetic susceptibility (χ_{lf}) and the isothermal remanent magnetization (IRM). The χ_{lf} in the soil profiles decrease from bedrock to intermediate soil horizons but notably increase towards top. Spatial variations based on the fundamental rock magnetic parameters (χ_{lf} and their frequency dependency (χ_{fd}), saturation IRM, demagnetization ratio) and knowledge of the polluting sources show significant anthropogenic loading for the topsoils. The study further reports remarkable post-monsoon changes in all the parameters controlled by surface run-off due to slope variation which appears to be the most effective mechanism of redistribution and dumping the topsoils loaded with anthropogenic particulate matters. Distribution of χ_{fd}% further infers wind as another important agent for dispersal of finer ferrimagnetic particulate matters predominantly controlled by the topography amongst other meteorological factors. Additional data for succeeding years would help in modelling the redistribution sensitivity and heavy metal residence effect for the topsoils and sediments in the PMR region.

Keywords: Anthropogenic loading, particulate matters, rock magnetism, soils.

SURFACE loading of anthropogenic dust and aerosol particulate matters (PM) play an important role in deteriorating the natural qualities of soil, water and air in the urban and industrialized areas. Knowledge of the distribution and residence (by surface loading) of anthropogenic particulates and understanding the re-distribution mechanism through atmospheric agencies like precipitation and wind circulation is essential to determine the extent to which the deterioration has occurred and also to envisage the long term residence effects in soil and water. Surface topography and prevailing wind conditions are the key factors of initial control over the distribution and redistribution of the topsoils along with PM. Discrimination of the anthropogenic from lithogenic (geogenic) components of the topsoils is therefore crucial in estimation of the anthropogenic loading in the urban and industrialized zones.

Urban soils are recipients of large amount of heavy-metal-rich dust from a variety of sources including industrial waste, vehicular emission, coal burning and other human activities. Heavy metal study in the urban soils therefore acts as useful criteria for investigating environmental pollution. A direct and empirical relationship between heavy metal concentration and mineral magnetic parameters has been widely reported from various case studies[1–14]. Magnetic methods are particularly favoured due to their several advantages over geochemical methods amongst its non-destructive nature, rapid analysis to produce a large qualitative and quantitative database, and relatively inexpensive nature of analysis[15–18]. These methods are particularly useful in estimating the concentration and distribution besides discrimination of magnetic minerals in natural and urban environments. However, knowledge of the source of magnetic susceptibility signals is essential to infer the anomaly and relate with pollution studies; which can be readily explored through routine rock magnetic analysis. The present study is therefore aimed at finding out the magnetic susceptibility distribution for topsoils in the Pune Metropolitan Region (PMR) during pre- and post-monsoon periods to understand the style of distribution and the mechanism of re-distribution of the anthropogenic loading, with a sampling grid of ~3 × 3 km.

Background

Anthropogenic dust arising from fossil fuel burning and industrial emissions can result in massive injection of

*For correspondence. (e-mail: sangode@unipune.ernet.in)

mineral aerosols into the atmosphere[8,19–22]. The resulting climatic effect is comparable to that from clouds[23] and it significantly affects the cycles of N, S and atmospheric oxidants[24]. An annual average of 40% (locally reaching 70%) of the total sulphate is associated with mineral dust over Asia, the Western United States, Australia and North Africa and large parts of the oceans have over 10% of sulphate associated with mineral aerosols[25]. Recently, Gaffney and Benjamin[26] produced a Pune Regional Emission Inventory to identify the most important sources of PM-air pollution in the entire Pune district. They developed a broad PM emission inventory by accounting for the sources of particulate emission and the quantity of PM emitted by each source, indicating that air quality in Pune district is greatly impacted by PM besides pollutants such as oxides of nitrogen (NO_x) and volatile organic compounds. Their[26] estimate for Pune district PM_{10} emission has shown that the significant sources of PM-air pollution are agricultural land preparation operations, paved and unpaved road dust, brick kilns and vehicular exhaust emission. These studies further point out that the agricultural emission would be a much smaller contributor to the local PM_{10} emission estimates directly within the city and obviously more of the point sources like industry and vehicles are expected to contribute significantly in the metropolitan region.

Heavy metal concentration and magnetic parameters linkages

Large quantities of heavy metals from a variety of sources including industrial waste and emission, vehicular emission, coal burning and fly ashes contain a significant amount of ferrimagnetic minerals characteristic of source[1,2,6,8,27]. Magnetic and heavy metal concentration can often be correlated although several factors may dilute the linkages between them[13]. The direct relation may be either due to incorporation of heavy metals into the lattice structures of Fe-rich fly-ash particles in the fossil fuels during combustion or subsequent incorporation of heavy metals onto the surface of ferri-/antiferro magnetic carriers present in the soils[13]. However, the data based relationship between heavy metals and magnetic parameters in the soils, dust and aerosols is particularly strong[2–5,10–12,28–33]. Pyrite and other iron impurities in the pulverized coals are transformed into molten spherules of magnetic iron oxides (i.e. magnetite, maghemite, haematite and their mixtures) and iron, liberating SO_x as gaseous components[5,10,30,34]. Thus, a fraction of iron is ultimately converted into ferrimagnetic minerals, which are in turn emitted into the atmosphere together with other phases[34]. Depending on the shape and size, the anthropogenic ferromagnetic minerals from stack emission are transported as dust or aerosols over variable distances before being deposited on the soil surface[35]. One of the mechanisms proposed is surface adsorption of metal oxide (magnetic phases) during fly ash formation[36–38]. Some workers also refer to a preferential adsorption of Pb, Zn, Cu, Cr, Cd on the surface of iron(III) oxyhydroxides as an alternative mechanism to describe the association with heavy metals. In various studies, the relationship between magnetic susceptibility and heavy metal concentration was further explored by using advanced statistical methods like Fuzzy C-means cluster analysis in the areas of multiple pollution sources[28,29,39–41]. The magnetic susceptibility values along highways are found to be positively correlated with heavy metals, in particular Pb, Cu, Cd and Zn; and the magnetic particles are often found agglomerated with lead[10,42].

Magnetic properties therefore can be effectively used as 'proxy' for estimating the contamination in various natural systems. The close relationship of magnetic susceptibility with heavy metal contamination in majority of the cases has been proved by combined analysis of chemical and magnetic data (*op. cit*). Some of them show that the magnetic particles and heavy metals are produced independently by the same process[5]. Yet the relationship amongst the magnetic properties and pollutants are complex and they are characteristic for each industrial or vehicular process demanding detailed investigation for the given case study.

The Pune Metropolitan Region

Pune is situated near the western margin of the Deccan basaltic province at the leeward side of the Western Ghats. It is a broad open valley at a height of about 560 m above msl in the upper Bhima basin and is traversed by the Mula, Mutha and Pavna rivers. The city is surrounded by hills to its eastern and southern sides and the Katraj–Diveghat range makes its southernmost boundary (Figure 1). The highest elevation point within the city is Vetal hill (800 m) and that in the outskirts is Sinhgad fort (1400 m). The city centre is located near the confluence of Mula and Mutha rivers. The other main river approaching the city is Pavna entering from the northern side of the city and joins the Mula river at a place called 'Dapodi' (Harris Bridge). After this confluence, the Mula river meanders towards the city centre and meets Mutha river which comes from the SW part of the city. The confluence of Mula–Mutha rivers occurs near the Engineering College (COEP/Sangam Bridge), turns eastward and is named as Mula–Mutha river. Some canals are also present in the city out of which Mutha right bank is the most important, providing water to the southern part of the city. Another canal (New Canal) joins the Mutha right bank canal in Koregoan Park near the race course. Apart from the canal and the main rivers, Pune is surrounded by some major/minor irrigation projects such as Khadakvasala, Panshet, Varasgoan, Bhatghat and Virchaskaman.

All these projects act as major sources of drinking and irrigation water for the city and adjoining areas. Some small lakes are also present within and outside the city like Pashan lake, Vishrantwadi lake, Mastani lake and Katraj lake. These lakes are also a source of drinking and irrigation water.

The PMR includes Pune urban area, Pimpri–Chinchwad Corporation, Khadki and Dehu Road cantonment and a few semi-urbanized villages on its periphery. The Pune city urban area is extended to 700 sq. km, whereas the PMR is 1605 sq. km. Once called the cycle city during the 1970s, Pune has grown into a metropolis with high vehicle density, major industries and growing population.

Climate

Pune has a typical monsoon climate with three distinct seasons like the rest of the country. The above mean sea level altitude, the leeward location of the city with reference to Western Ghats and the sea breeze make the city's climate moderate. The mean maximum and minimum temperatures for the hottest month (May) are 37°C and 23°C and that for the coldest month (December) are 30°C and 12°C respectively. The relative humidity ranges from 36% in the month of March to 82% in August. Three-fourths of the annual rainfall of 70 cm occurs in four months from June to September.

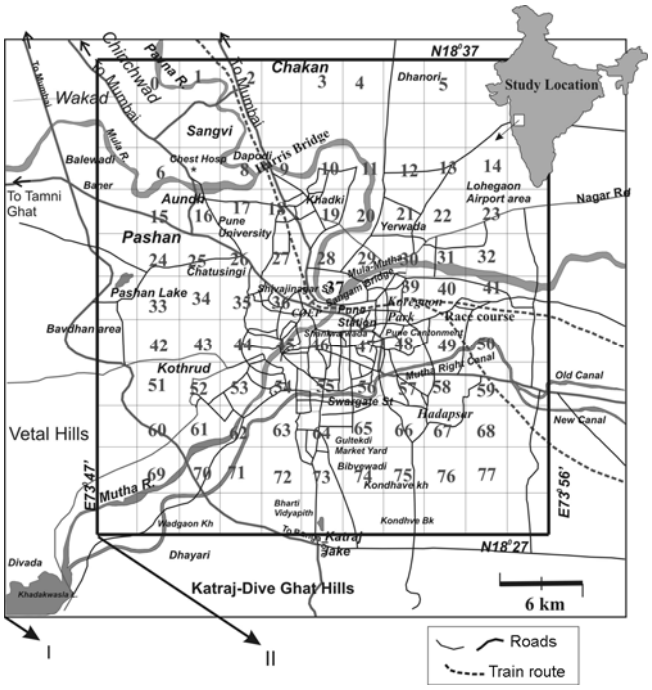

Figure 1. The study area map prepared with the help of www.wikimapia.org, showing the important localities, roads and other features quoted in the text. The rectangle marked 'I' is the grid area used for producing the digital elevation, contour and slope maps (as in Figures 2 and 3) in a 2×2 km grid; whereas the area marked 'II' is the actual sampling sites (numbered) used for the analysis adopting a 3×3 km grid.

Fieldwork, sampling and laboratory analysis

A latitude/longitude controlled map with 2 sq. km grid covering an area of 1760 sq. km for the PMR is prepared with the help of *Wikimapia* and *Google Earth* (see Figure 1). A contour map and digital elevation model is prepared using Surfer-7 software by assigning the average heights for each grid (Figure 2 *a* and *b*). The Pune city centre corresponds to a relative depression and the confluence area for Mula and Mutha rivers surrounded by isolated hills and hillocks. Mula, Mutha and Pavna rivers carve out distinct valleys for major part of the PMR (see Figure 2). A slope vector map is generated using Surfer-7 (Figure 2 *a*) in which an arrow marks the slope direction, and the length of segment is proportional to the slope gradient. Slopes in the S, SW and NW quadrants are undulating while they are gentle in the NE corner. The effect of slope on magnetic variable is discussed in the results.

Since the 2×2 km grid used for the DEM and slope maps (Figures 1 and 2) is too close as sampling interval for the present study; a 3×3 km grid was adopted for the pre- and post-monsoon soil sampling (see Figure 1 (II)). Topsoils (<15 cm) and the bedrocks were sampled from open grounds, gardens, parks, roadsides and forest areas within the predefined square grid pattern. In order to assess the contribution from natural sources (pedogenic/lithogenic), four sections of soil profiles, and two flood plain deposits of Pavna and Mula rivers have been studied in detail. Further, to avoid site specific bias, three samples were collected from each grid and mixed by coning and quartering. Rainwater samples were collected during monsoon periods at selected sites for a period of 35 days from 15 June to 20 July 2007 in 15 litre buckets.

Soil samples were lightly crushed and homogenized by coning and quartering and packed in three non-magnetic pots each by wrapping in cling films. Low and high frequency (0.47 and 4.7 kHz) magnetic susceptibility measurements were made for each pot by repeating 6 times each frequency using MS-2B Bartington magnetic susceptibility meter. This is followed by the isothermal remanent magnetization (IRM) analysis (described here). All the rock magnetic analyses are performed at the K.S. Krishnan Geomagnetic Research Laboratory (IIG), Allahabad.

Magnetic susceptibility

Magnetic susceptibility in the environmental samples is the sum total of the susceptibilities of ferro-, ferri-, antiferro-, para- and diamagnetic constituents[15]. Using a low external magnetic field (<250 μT), the influence of ferro- and ferrimagnetic components can be ascertained by blocking the effects for others[16]. A frequency dependent susceptibility measurement involves detecting ultrafine ferrimagnetic (also called super paramagnetic

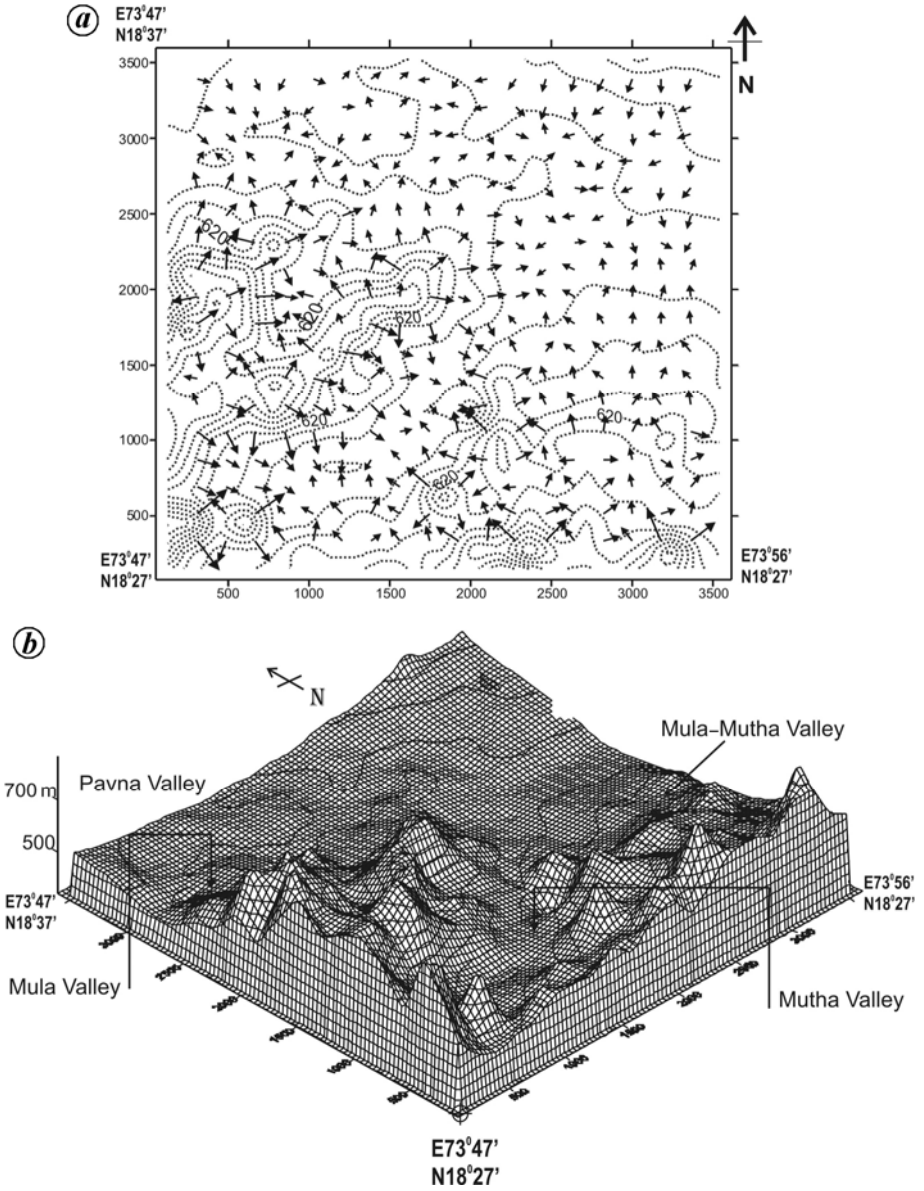

Figure 2. ***a***, Contour map along with the slope vector data prepared using the 2×2 km grids of area 'I' mentioned in the Figure 1. The vectors are in the direction of slope with its length proportional to the slope gradient intensity. ***b***, Digital elevation map (DEM) for the same grid in the rectangular area of 'I' as above. Both these maps generated using Surfer-7 software.

(SP) fraction of <0.03 μ) and to some extent the single domain (SD ≃ >0.03 to <0.06 μ fraction) by using two or more frequencies (e.g. 0.47 and 4.7 kHz) at the constant low applied field[15,16]. Higher frequency (4.7 kHz) measurements do not allow SP grains to react with the applied external field, as it changes more quickly than the required relaxation time for SP grains. As a result, in the higher frequency, lower values of susceptibility are encountered and the difference is equated to estimate the SP ferrimagnetic particles. Mathematically, it can be expressed as $\chi_{fd}\% = \{(\chi_{lf} - \chi_{hf})/\chi_{lf} \times 100\}$, where χ_{lf} is low frequency (0.47 kHz) susceptibility and χ_{hf} is of higher frequency (4.7 kHz).

Isothermal remanent magnetization

Remanent magnetism arising out of the short-term exposure to strong magnetizing fields at constant temperatures known as IRM is measured at room temperatures in forward (acquisition up to 1000 mT) and reverse (demagnetization up to –300 mT) directions of the applied field producing the remanance hysteresis loops for each specimen. SIRM is the field at which saturation in IRM acquisition occurs, and it depends upon the composition, microstructure and concentration of the magnetic minerals in a specimen[43]. Coercivity of remanence (B_{CR}) is the demagnetizing factor, where SIRM is completely demag-

netized. It is used to identify the magnetic mineral composition when ferri- as well as canted antiferromagnetic minerals are present or is sensitive to grain size (domain size) when the ferrimagnetic minerals alone are present as in the present case[18,43,44].

Results and discussion

Average soil cover in the PMR region varies from 0 to 3 m, and more commonly in between 10 and 30 cm in the city area. The topsoil colours vary from dark brown (7.5 YR) to black (10 YR) in the standard Munsell notations[45]. As the iron oxides play a fundamental role in imparting the characteristic colours to the soils, a soil colour map based on Munsell notations is prepared for the topsoils in the sampled grid area (Figure 3), to relate them with studied magnetic parameters. The soil colour shows very dark brown (7.5 YR 2.5/2 to 2.5/3) to dark brown (7.5 YR 3/2 to 3/4) in the NE corner and some of the central parts of the PMR. The hilly areas in S, W and SW show large variations from yellowish brown (10 YR 4/6) to dark red (2.5 YR 5/1). Areas near the channels with water logging conditions show dark grayish brown (10 YR 4/2), reddish grey (2.5 YR 5/1) and black (10 YR 2/2) colours.

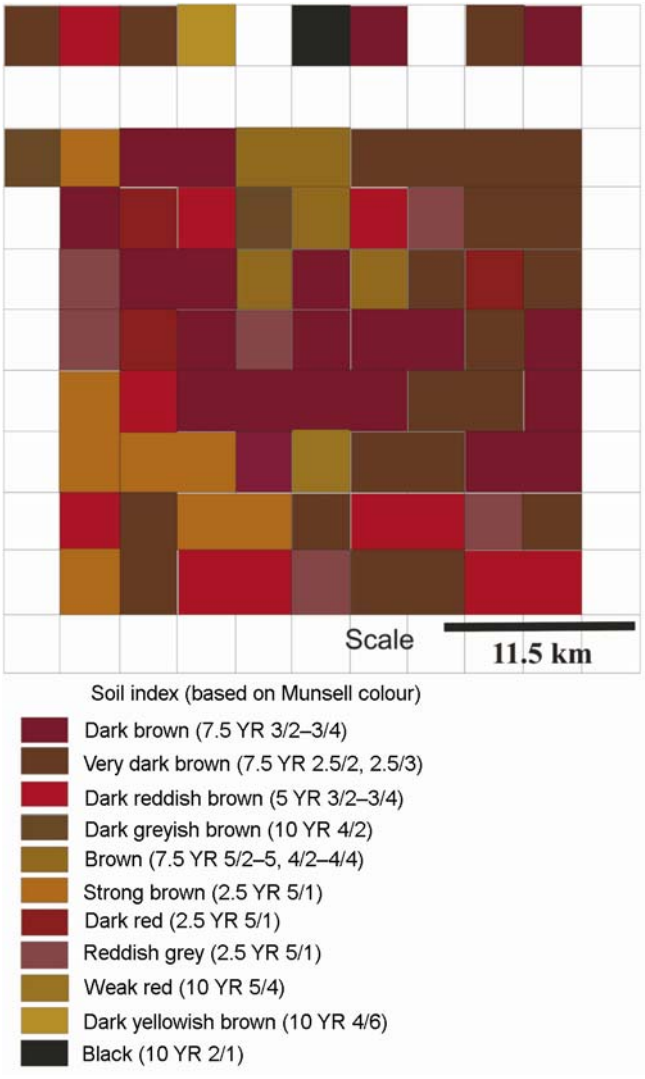

Figure 3. A soil colour map for the PMR region developed by using the Munsell colour charts (Munsell[45]) for the sampled grid area-II.

We sampled the soil profiles from bedrock (parent) to topsoils to see the variation in magnetic susceptibility. An ideal profile in the grid number 77 has been studied in detail for the field observations and rock magnetic properties (see Figure 4). It shows that the susceptibilities and frequency dependence increases in the immediate soil horizons while it drops in the intermediate horizon. Then the susceptibility and SIRM increases towards top with simultaneous decrease in the coercivity and frequency dependency. This shows increasing influx of the coarser ferrimagnetic fraction for the topsoils that can be of detrital and/or anthropogenic nature. We further study the spatial patterns to infer the influx in topsoils. The mean mass normalized susceptibilities (χ_{lf}) shows higher values for the bedrocks and decrease in order from the pre-monsoon soil > dust > rainwater filtrates (Table 1). It is also noted that the χ_{lf} (as well as χ_{fd}%) shows significant decrease (>20%) for the post-monsoon soils. This suggests either the dilution of topsoils by addition of new, less ferrimagnetic material or the removal/erosion of topsoils. Both these possibilities are further studied by spatial plots of Surfer (Figures 5–8) and discussed here. No significant difference is found in the statistical means of fundamental rock magnetic properties such as *S*-ratio and B_{CR} for the average values of the pre-monsoon soils, bedrocks, dust and rain water samples that suggest predominantly ferrimagnetic mineralogy with SD–MD domain size. However the concentration dependent parameters (SIRM and χ_{lf}) show discrete values for each of the sampling domains. The fundamental rock magnetic parameters (χ_{lf}, χ_{fd}%, SIRM and *S*-ratio) for pre- and post-monsoon periods are therefore described in integration to topography, slope map and the locality characteristics in the Figures 5–8.

Comparison of pre- and post-monsoon soil susceptibilities (Figure 5) shows that a major peak for the pre-monsoon soils in the NW corner of the Chinchwad and Wakad area has been notably reduced for post-monsoon soils. The DEM (Figure 2) shows this area as a relatively low lying region between Mula and Pavna valleys. Two major highways of heavy traffic (Pune–Mumbai and the Expressway) converge in this region that suggests loading by PM related to vehicular dust. Slope map (Figure 2) shows gentle slopes towards SE in this area suggesting the surface run-off during monsoon as a major control of redistribution. Further, there is a dome shaped peak at the Sangam Bridge and Pune Railway Station area for the pre-monsoon soils which diminishes during

Table 1. Descriptive statistics for the fundamental rock magnetic parameters (χ_{lf}: mass normalized susceptibility in 10^{-8} m^3/kg, χ_{fd}%: frequency dependence of susceptibility percentage, B_{CR}: coercivity of remanance in mT and SIRM: saturation remanance magnetization in 10e–5 Am^2/kg), separately exercised for the pre- and post-monsoon soils, bedrocks, dust and rainwaters

	χ_{lf} pre-soil	χ_{fd}% pre-soil	χ_{lf} post-soil	χ_{fd}% post-soil	χ_{lf} bedrock	χ_{fd}% bedrock	B_{CR} pre-soil	SIRM pre-soil	*S*-ratio pre-soil	B_{CR} bedrock	SIRM bedrock	*S*-ratio bedrock
Soil and bedrock												
Mean	78.61	2.40	59.78	1.35	79.78	3.96	39.23	18,505.81	–0.57	40.08	26,340.32	–0.51
Median	65.76	1.64	55.72	1.17	54.84	2.09	40.00	10,625.20	–0.56	50.00	19,843.84	–0.51
SD	46.24	3.81	25.75	0.96	66.87	5.82	11.86	20,746.13	0.14	13.95	20,538.92	0.22
Kurtosis	10.99	22.91	1.32	–0.06	2.62	17.07	–1.28	5.14	3.33	–1.50	2.81	–0.52
Skewness	2.73	4.51	0.90	0.70	1.76	3.75	–0.14	2.46	0.61	–0.29	1.72	0.05
Minimum	21.66	0.20	18.49	0.00	13.63	0.00	20.00	3,351.10	–0.91	20.00	6,384.34	–0.92
Maximum	303.61	24.00	146.03	3.80	272.94	32.51	60.00	90,322.28	–0.05	64.00	90,897.27	–0.05

	χ_{lf}	χ_{hf}	χ_{fd}	χ_{fd}%	B_{CR}	*S*-ratio
Dust						
Mean	59.57	59.82	–0.26	–0.41	52.00	–0.31
Median	56.47	56.18	–0.46	–0.83	47.00	–0.30
SD	12.44	12.62	0.48	0.82	3.33	0.05
Minimum	48.97	49.43	–0.60	–0.94	36.00	–0.49
Maximum	73.26	73.86	0.30	0.53	53.00	–0.30

	χ_{lf}	χ_{hf}	χ_{fd}	*S*-ratio	B_{CR}
Rainwater					
Mean	10.60	10.62	3.96	–0.60	42.48
Median	8.93	9.60	0.00	–0.59	42.50
SD	5.76	5.74	5.82	0.04	3.11
Minimum	1.87	2.13	0.00	–0.73	32.00
Maximum	22.67	21.87	22.50	–0.55	47.00

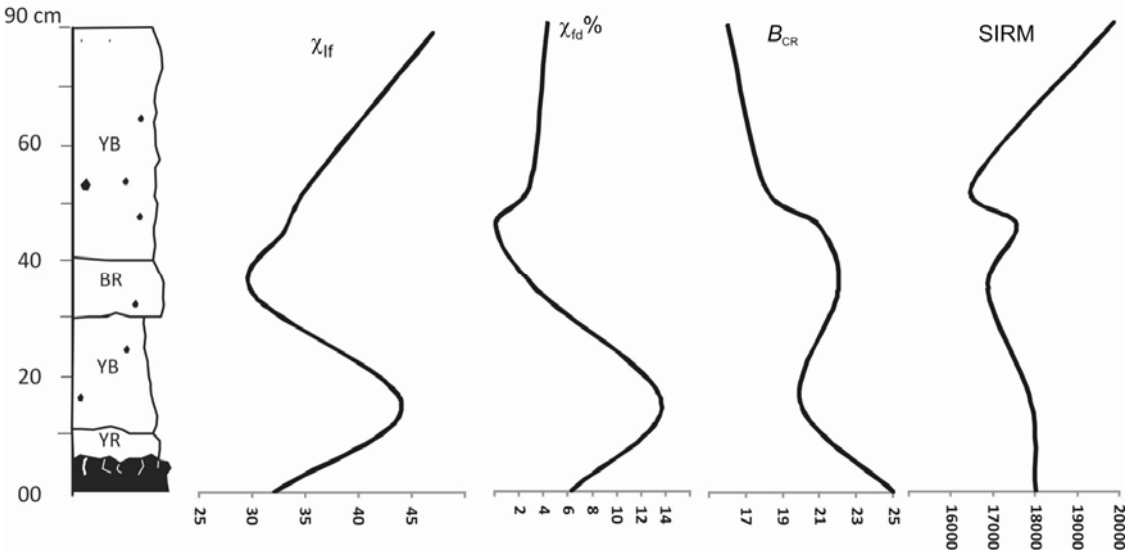

Figure 4. A typical soil profile in the sampled grid area (in the grid no. 77 of Figure 1) analysed for detailed rock magnetic study. It shows a large variation in all the properties with notable increase in the concentration of ferrimagnetic particles for the top soils. YB, yellowish brown; BR, brownish red; YR, yellowish red. The dark filled area at the bottom of the log shows the bedrock.

the post-monsoon period and a ridge shaped anomaly emerges during post-monsoon in the region from Kothrud, Swargate to Pune Cantonment area. This anomaly coincides with the eastward slopes converging with northward slope in the cantonment area producing a peak within the ridge suggesting the transportation and re-deposition of the anthropogenically loaded topsoils during rainy season. Another peak in χ_{lf} emerges at the

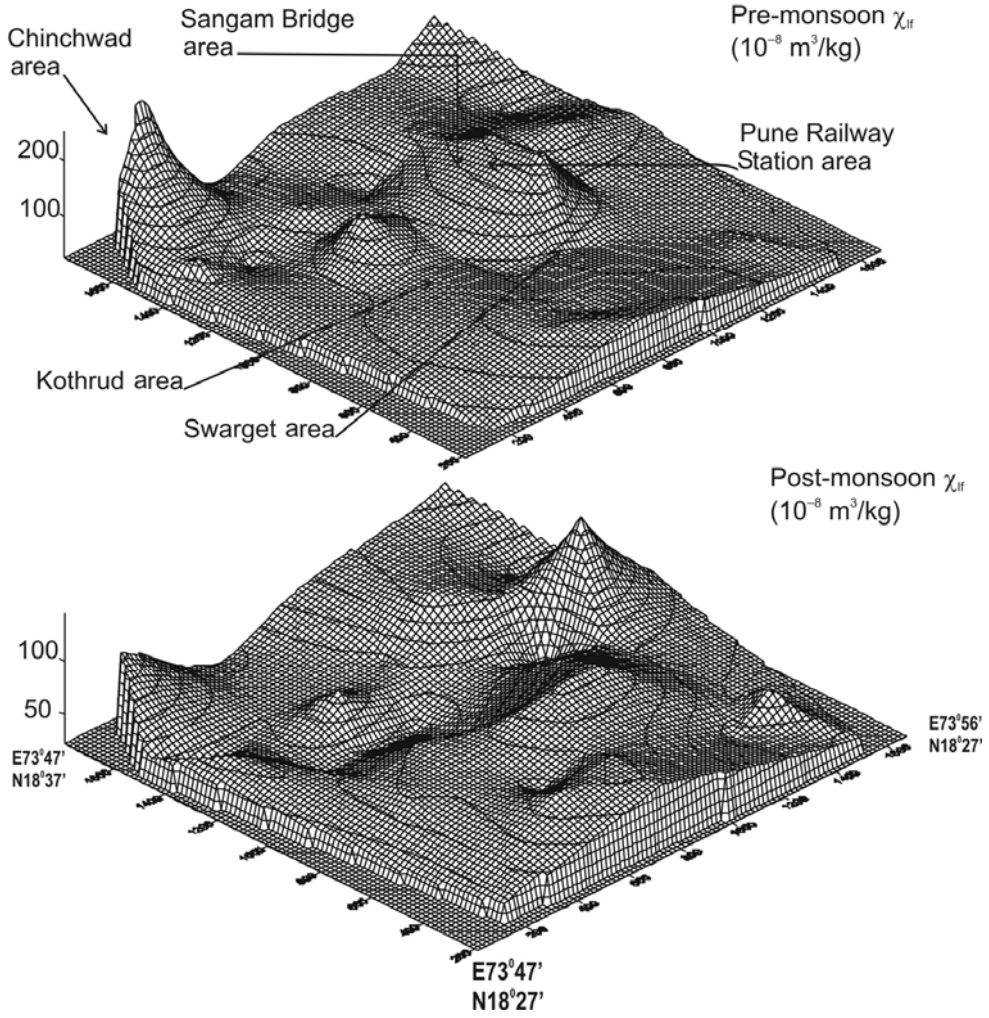

Figure 5. The elevation maps for mass normalized susceptibilities (χ_{lf}, 10^{-8} m^3/kg) showing distribution pattern for the soils of PMR over pre- and post-monsoon periods for the sites in the grid area II. Details on variation in the susceptibility pattern is discussed in text.

NE corner for the pre-monsoonal soils. This peak occurs in the Alandi and Dehu road area which is heavily industrialized and has higher density of heavy and light vehicle traffic. The Dehu road also has a busy railway station. This suggests a heavy anthropogenic loading in the area giving rise to higher susceptibility values of the above peak. In the post-monsoon scenario, a conspicuous peak in χ_{lf} emerges in the Yerawada region (Figure 5). It can be noted that there was no peak in this area for the pre-monsoon soils. Considering the slope map, there is a confluence of three regional slopes: (a) from north, the Dehu–Alandi area, (b) from west, the Shivajinagar area and (c) from the SW, the Pune Railway Station and other heavy traffic areas. This suggests that the sediments/topsoils with ferrimagnetic materials during rainy season are transported from (a), (b) and (c); and re-deposited in the Yerwada region. These inferences suggest that the monsoon precipitation governed by surface slopes play an important role in the redistribution of the topsoils. Therefore the areas of merging two or more slopes are also the sites of major dumping of the anthropogenically loaded topsoils.

The frequency dependence of susceptibility (χ_{fd}), which is sensitive to the concentration of finer ferrimagnetic particles in the range of typically less than 0.06 μ[18,43,45] shows a notable pre-monsoon anomaly in the northeastern part near the old Mumbai–Pune road (the traffic junction for heavy as well as light vehicles). The other minor peak emerges in the south near the Solapur road which is again a mixed traffic junction of Hadapsar. There is significant modification in the post-monsoon soil χ_{fd}% with several new peaks and troughs emerging. More noticeable amongst this is the N–S ridge shaped anomaly in the eastern margin. It can be postulated that the prevailing strong eastward monsoonal winds might have carried the finer ferrimagnetic particles (to which χ_{fd} is sensitive) and deposited in this eastward direction producing the given pattern. The geometry of this ridge corresponds to

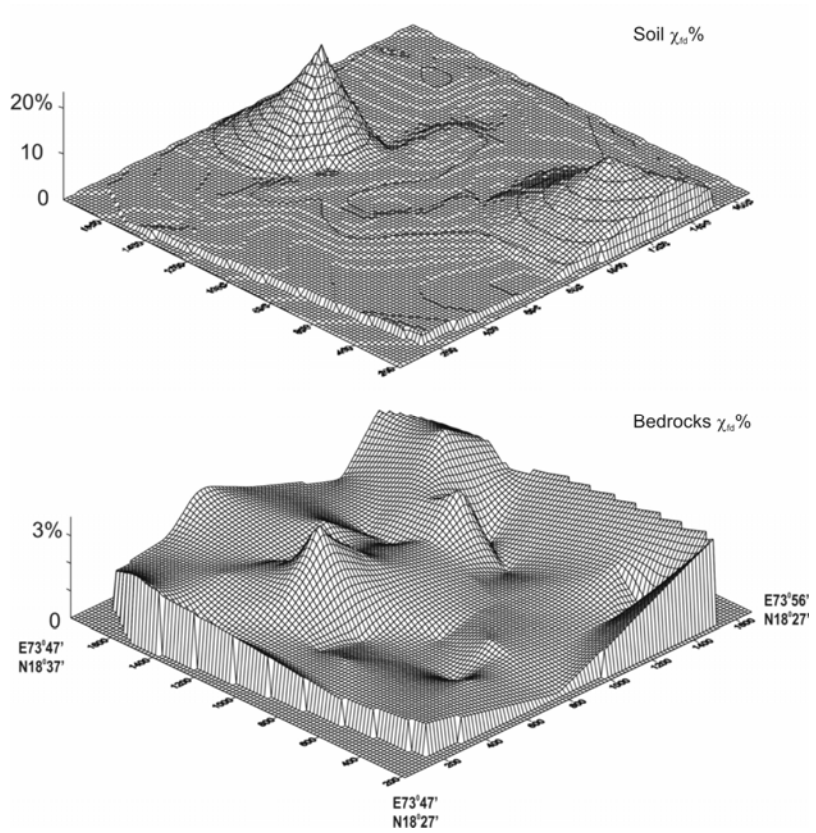

Figure 6. Elevation map for the percentage distribution of the frequency dependency of susceptibility for the pre- and post-monsoon soil samples in the grid area II.

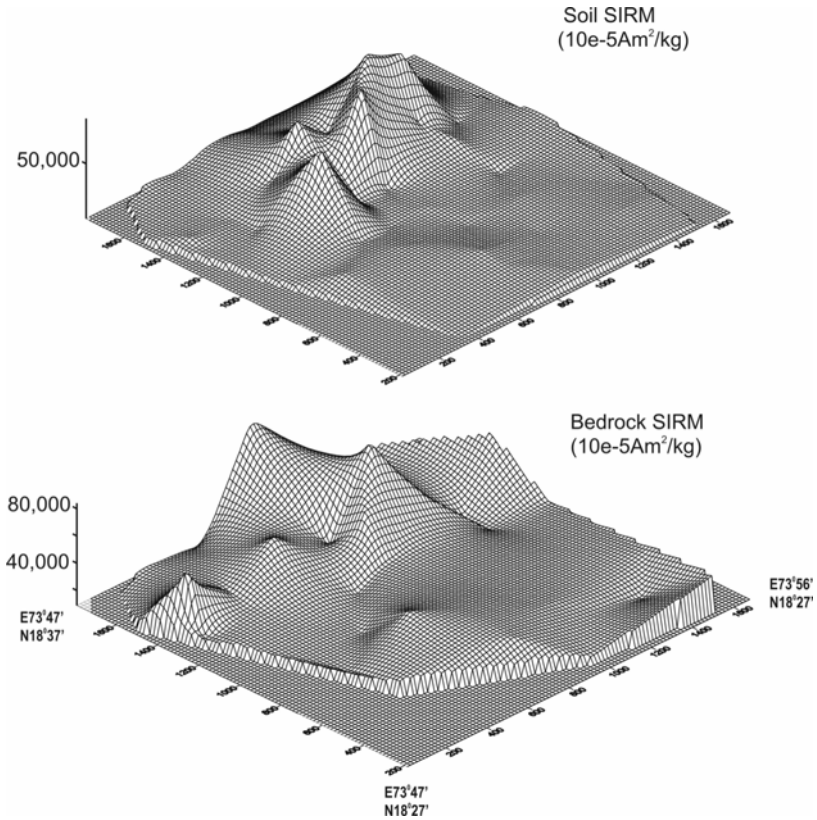

Figure 7. Elevation map for the concentration dependent parameters SIRM (mA/m) for the bedrock and pre-monsoon soils in the PMR region of the grid II.

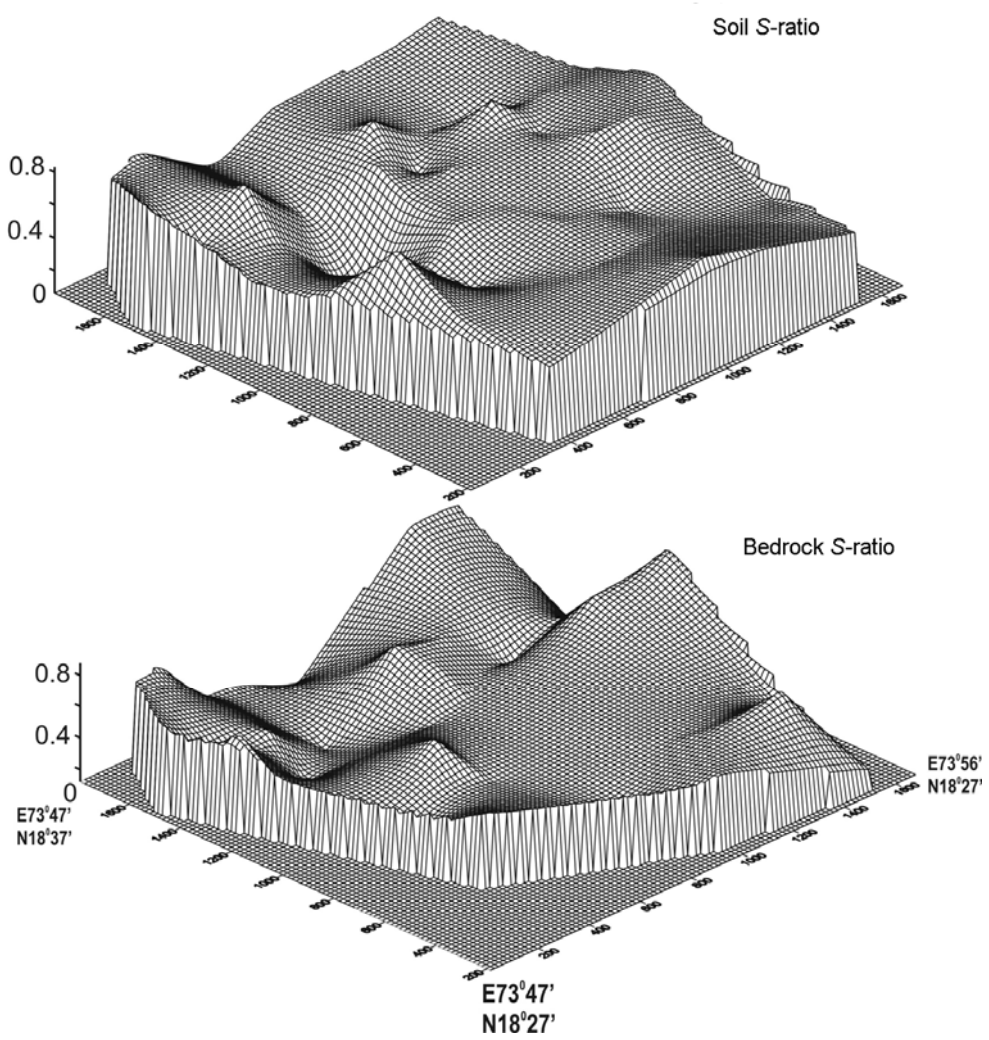

Figure 8. The *S*-ratio elevation map for the bedrocks and the pre-monsoon soils in the PMR region (grid II).

that of the topography of the area (see Figure 2) acting as a barrier to drop the particles. The χ_{fd}% therefore indicates that the monsoonal winds are the most effective redistributing agent for the finer ferrimagnetic particles (wind-blown dust) in the mountain slopes, where the mountain ridges act as barrier to wind currents.

Further in order to analyse the bedrock–soil relations, we plot the concentration dependent parameter (SIRM) and the mineralogy/grainsize dependent parameter (*S*-ratio) for the pre-monsoon soils and bedrocks (Figures 7 and 8 respectively). The SIRM in the bedrock shows variability especially in the northern part where pedogenesis and bedrock weathering is more prevalent compared to the southwestern and southern parts (Figure 7). The higher SIRM in the northern part therefore suggests enrichment due to weathering where the easily weathered weakly magnetic minerals like feldspar and quartz are removed. Although there are high SIRMs in the soils in the northern half, there is no one-to-one correlation between bedrock and soil susceptibilities. This suggests that the variation in topsoil magnetic parameters is independent of the immediate bedrock lithogenic variations indicating that either the transported nature of topsoils or input from clay particles is in the form of dust in the topsoils.

The coercivity of remanance (B_{CR}) and *S*-ratio are indicative of an overall predominance of the ferrimagnetic mineralogy for all the studied samples in the PMR region. In this instance the variation in *S*-ratio is broadly controlled by the variation in ferrimagnetic grainsize (Figure 8). The *S*-ratio shows relatively less peakedness but more undulations for the soils compared to the bedrocks. This probably indicates the re-distributing tendency for soils to normalize the peakedness.

Road profiling

In order to study the mineral magnetic variations due to vehicular activity, systematic sampling was conducted for the road profiles (normal to the roads, Figure 9) for some

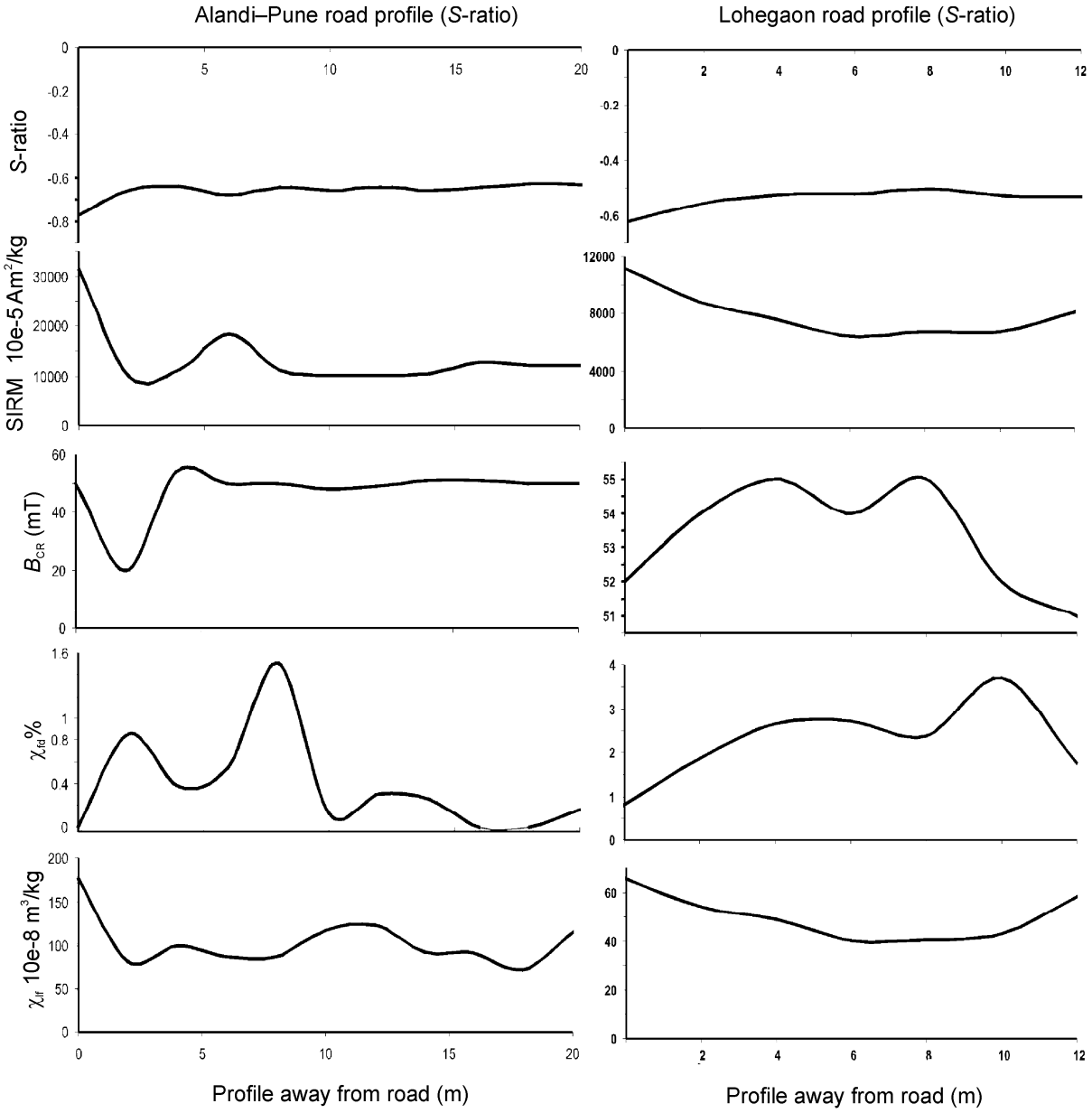

Figure 9. Variation in the soil rock magnetic properties sampled at 1 m interval for the two important roads in the PMR region.

of the heavy traffic areas in the city. Care has been taken to choose such roads where there was no rain and no sweeping activity at least for the last 2 months during summer. A profile of the Alandi–Pune road shows a sharp decrease in the concentration dependent parameters (χ_{lf} and SIRM) within first 4 m interval from the side of the road (Figure 9). However, the χ_{fd}% and *S*-ratio do not show any notable trend for this road. The B_{CR} shows a major drop within 2 m indicating that the concentration of larger ferrimagnetic grains is restricted within these 2 m of the road profile. The other road profile that was taken from one of the busy traffic areas near the Lohegaon airport also behaves in a similar manner with decreasing trend of concentration dependent parameters within 4–6 m from the roadside. Similarity in the behaviour of rock magnetic parameters for both the roads infers that the effective accumulation from the vehicular emission occurs well within 6 m from the roadsides. However detailed work is needed to relate the other variables like effect of slope, vehicle frequency, seasonal change and type of traffic, etc.

Conclusion

The present study indicates that an integrated bedrock-, topsoil-, dust- and rainwater sampling for the pre- and post-monsoon periods in a grid manner is the most effec-

tive method of soil magnetometry to assess the anthropogenic loading in the metropolitan regions. The bedrock and soil composition in the PMR region is mainly of ferrimagnetic nature and their concentration and grainsize in the topsoils is mainly governed by the anthropogenic loading and its redistribution. Surface water run-off during monsoon precipitation controlled by relief is the chief mechanism of redistribution of topsoils and sediments loaded with anthropogenic PM. Prevailing winds during summer and monsoon seasons appears to be another efficient agent for large scale dispersal of the finer ferrimagnetic particles (<0.06 μ). This too appears to be governed by the surface topography in the PMR area, where the wind flow direction is eastward. Further, the roadside topsoils and sediments in heavy traffic areas infer that majority of the ferrimagnetic concentrations occur within 6 m.

Work is in progress along with geochemical approach, aerosol sampling and source apportionment to develop a suitable model for redistributing sensitivity to seasonal changes and the residence tendency of the heavy metal PM in the PMR region.

1. Flanders, P. J., Collection, measurement, and analysis of airborne magnetic particulates from pollution in the environment. *J. Appl. Phys.*, 1994, **75**, 5931–5936.
2. Heller, F., Strzyszcz, Z. and Magiera, T., Magnetic record of industrial pollution in forest soils of Upper Silesia, Poland. *J. Geophys. Res*., 1998, **103**, 17767–17774.
3. Petrovsky, E., Kapicka, A., Zapletal, K., Sebestova, E., Spanila, T. and Dekkers, M. J., Correlation between magnetic parameters and chemical composition of lake sediments from northern Bohemia: preliminary study. *Phys. Chem. Earth*, 1998, **23**, 1123–1126.
4. Bityukova, L., Scholger, R. and Birke, M., Magnetic susceptibility as indicator of environmental pollution of soil in Tallinn. *Phys. Chem. Earth* (*A*), 1999, **24**, 829–835.
5. Kapicka, A., Petrovsky, E., Ustjak, S. and Machackova, K., Proxy mapping of fly-ash pollution of soils around a coalburning power plant: a case study in Czech Republic. *J. Geochem. Exp*., 1999, **66**, 291–297.
6. Kapicka, A., Jordanova, N., Petrovsky, E. and Ustjak, S., Magnetic stability of power-plant fly ash in different solutions. *Phys. Chem. Earth* (*A*), 2000, **25**, 431–436.
7. Hanesch, M. and Petersen, N., Magnetic properties of a recent parabrown-earth from Southern Germany. *Earth Planet Sci. Lett*., 1999, **169**, 85–97.
8. Hoffmann, V., Knab, M. and Appel, E., Magnetic susceptibility mapping of roadside pollution. *J. Geochem*., 1999, **66**, 313–326.
9. Xie, S., Dearing, J. A., Boyle, J. F., Bloemendal, J. and Morse, A. P., Association between magnetic properties and element concentrations of Liverpool street dust and its implications. *J. Appl. Geophys*., 2001, **48**, 83–92.
10. Hanesch, M. and Scholger, R., Mapping of heavy metal loadings in soils by means of magnetic susceptibility measurements. *Environ. Geol*., 2002, **42**, 857–870.
11. Chaparro, M. A. E., Gogorza, C. S., Lavat, A., Pazos, S. and Sinito, A. M., Preliminary results of magnetic characterization of different soils in Tandil region (Argentina) affected by the pollution of metallurgical factory. *Eur. J. Environ. Eng. Geophys*., 2002, **7**, 35–58.
12. Chaparro, M. A. E., Gogorza, C. S. G., Chaparro, M. A. E., Irurzun, M. A. and Sinito, A. M., Review of magnetism and heavy metal pollution studies of various environments in Argentina. *Earth Planets Space*, 2006, **58**, 1411–1422.
13. Chaparro, M. A. E., Bigegain, J. C. and Sinito, A. M., Magnetic studies applied to different environments (soils and stream sediments) from a relatively polluted area in Buenos Aires Province, Argentina. *Environ. Geol*., 2004, **45**, 654–664.
14. Maiti, S., Meena, N. K., Sangode, S. J. and Chakrapani, G. J., Magnetic susceptibility studies of soils in Delhi. *Geol. Soc. India*, 2005, **66**, 667–672.
15. Thompson, R. and Oldfield, F., *Environmental Magnetism*, Allen and Unwin, London, 1986, p. 220.
16. Collinson, D. W., *Methods in Rock Magnetism and Palaeomagnetism: Techniques and Instrumentation*, Chapman and Hall Publication, 1987, p. 503.
17. Walden, J., Oldfield, F. and Smith, J. P. (eds), *Environmental Magnetism: A Practical Guide*, No. 6, Quaternary Research Association, London, 1999, p. 243.
18. Evans, M. E. and Heller, F., *Environmental Magnetism: Principles and Applications of Enviromagnetics*, International Geophysics Series, Academic Press, 2003, vol. 86, p. 293.
19. Bhaskaran, B. and Mitchell, J. F. B., Simulated changes in southeast Asian monsoon precipitation resulting from anthropogenic emissions. *Int. J. Climatol*., 1998, **18**, 1455–1462.
20. Carmichael, G., Streets, D. G., VanAardenne, J. and Arndt, R. L., Anthropogenic fossil fuel sulfur and nitrogen emissions and sectorial in Asia. Proceedings of a Synthesis Workshop on Greenhouse Gas Emissions, Aerosols, Land Use and Cover Changes in Southeast Asia (ed. Moya, T. B.), China–Taipei, 1997, p. 124.
21. Ramanathan, V. *et al.*, Indian Ocean experiment: an integrated analysis of the climate forcing and effects of the great Indo-Asian haze. *J. Geophys. Res*., 2001, **106**, 28,371–28,398.
22. Gajghate, D. G. and Bhanarkar, A. D., Characterisation of particulate matter for toxic metals in ambient air of Kochi City, India. *Environ. Monit. Assess.*, 2005, **102**, 119–129.
23. Sokolik, I. N. and Toon, O. B., Direct radiative forcing by anthropogenic airborne mineral aerosols. *Nature*, 1996, **381**, 681–683.
24. Andreae, M. O. and Crutzen, P. J., Atmospheric aerosols: biogeochemical sources and role in atmospheric chemistry. *Science*, 1997, **276**, 1052–1056.
25. Dentener, F. J., Carmichael, G. R., Zhang, Y., Lelieveld, J. and Crutzen, P. J., Role of mineral aerosol as a reactive surface in the global troposphere. *J. Geophys. Res.*, 1996, **101**, 22869–22889.
26. Gaffney, P. and Benjamin, M., *Pune Regional Emissions Inventory Study* (*PREIS*), 2004; Available on www.unipune.res.in
27. Blundell, A., Hannam, J. A., Dearing, J. A. and Boyle, J. F., Detecting atmospheric pollution in surface soils using magnetic measurements: a reappraisal using an England and Wales database. *Environ. Pollut.*, 2009, **157**, 2878–2890.
28. Dekkers, M. J. and Pietersen, H. S., Magnetic properties of low-Ca fly ash: a rapid tool for Fe-assessment and a survey for potentially hazardous elements. *Mater. Res. Soc. Symp. Proc*., 1992, **245**, 37–47.
29. Durza, O., Heavy metals contamination and magnetic susceptibility in soils around metallurgical plant. *Phys. Chem. Earth* (*A*), 1999, **24**, 541–543.
30. Magiera, T. and Strzyszcz, Z., Ferrimagnetic minerals of anthropogenic origin in soils of some Polish national parks. *Water, Air Soil Pollut*., 1999, **124**, 37–48.
31. Shilton, V. F., Booth, C. A., Smith, J. P., Giess, P., Mitchell, D. J. and Williams, C. D., Magnetic properties of urban street dust and their relationship with organic matter content in the West Midlands, UK. *Atmos. Environ.*, 2005, **39**, 3651–3659.
32. Xue, S., Wang, S. and Yong, Q., Correlation between magnetic susceptibility and heavy metals in urban topsoil: a case study from the city of Xuzhou, China. *Environ. Geol*., 2005, **49**, 10–18.

33. Spiteri, C., Kalinski, V., Rosler, W., Hoffmann, V. and Appel, E., Magnetic screening of a pollution hotspot in the Laustitz area, E. Germany: proxies and heavy metal contaminations in soils. *Environ. Geol.*, 2005, **49**, 1–9.
34. Magiera, T., Strzyszcz, Z., Kapicka, A., Petrovsky, E. and MAGPROX Team, Discrimination of lithogenic and anthropogenic influences on topsoil magnetic susceptibility in Central Europe. *Geoderma*, 2006, **130**, 299–311.
35. Dedik, A. N., Hoffmann, P. and Ensling, J., Chemical characterization of iron in atmospheric aerosols. *Atmos. Environ. Part A*, 1992, **26**, 2545–2548.
36. Georgeaud, V. M., Rochette, P., Ambrosi, J. P., Vandamme, D. and Williamson, D., Relationship between heavy metals and magnetic properties in a large polluted catchment: the Etang de Berre (South of France). *Phys. Chem. Earth*, 1997, **22**, 211–214.
37. Hansen, J., Johnson, D., Lacis, A., Lebedeff, S., Lee, P., Rind, D. and Russell, G., Climate impact of increasing atmospheric carbon dioxide. *Science*, 1981, **213**, 957–966.
38. Hunt, A., Jones, J. and Oldfield, F., Magnetic measurements and heavy metals in atmospheric particulates of anthropogenic origin. *Sci. Total Environ.*, 1984, **33**, 129–139.
39. Beckwith, P., Ellis, J., Revitt, D. and Oldfield, F., Heavy metal and magnetic relationships for urban source sediments. *Phys. Earth Planet. Inter.*, 1986, **42**, 67–75.
40. Strzyszcz, Z. and Magiera, T., Distribution of ferromagnetics in forest soils of some Polish and German regions in relation to their origin. *Mitteilungen der Deutschen Bodenkundlichen Gesellschaft*, 1993, **72**, 1309–1312.
41. Hanesch, M., Scholger, R. and Dekkers, M. J., The application of fuzzy C-means cluster analysis and non-linear mapping to a soil data set for the detection of polluted sites. *Phys. Chem. Earth* (*A*), 2001, **26**, 885–891.
42. Knab, M., Appel, E. and Hoffmann, V., Separation of the anthropogenic portion of heavy metal contents along a highway by means of magnetic susceptibility and fuzzy C-means cluster analysis. *Eur. J. Environ. Eng. Geophys.*, 2001, **6**, 125–140.
43. Dunlop, D. J. and Ozdemir, O., *Rock Magnetism: Fundamentals and Frontiers*, Cambridge University Press, Cambridge, 1997, p. 573.
44. Thompson, R. and Oldfield, F., *Environmental Magnetism*, Allen and Unwin, London, 1986, p. 227.
45. Munsell, *Munsell Soil Color Charts*, Gretag Macberth, New York, 2000.

ACKNOWLEDGEMENTS. This work was funded by UGC grant and ISRO-UOP grant. We are grateful to the Director, Indian Institute of Geomagnetism, Panwel and the Head, Department of Geology (University of Pune) for providing the facilities. We are also grateful for the help extended by Ashwini Supekar, Hemant Jagtap, Deepali Rasal, Devdat Upasni during collection of rainwater samples. Two anonymous referees are acknowledged for critical comments and greatly improving the manuscript.

Received 10 October 2008; revised accepted 23 December 2009